

Ensemble properties of high frequency data and intraday trading rules

Fulvio Baldovin, Francesco Camana, Michele Caraglio, and Attilio L. Stella
*Dipartimento di Fisica e Astronomia, Sezione INFN, CNISM,
Università di Padova, Via Marzolo 8, I-35131 Padova, Italy*

Massimiliano Caporin
*Dipartimento di Scienze Economiche ed Aziendali,
Università di Padova, Via del Santo, I-35123 Padova, Italy*

Regarding the intraday sequence of high frequency returns of the S&P index as daily realizations of a given stochastic process, we first demonstrate that the scaling properties of the aggregated return distribution can be employed to define a martingale stochastic model which consistently replicates conditioned expectations of the S&P 500 high frequency data in the morning of each trading day. Then, a more general formulation of the above scaling properties allows to extend the model to the afternoon trading session. We finally outline an application in which conditioned forecasting is used to implement a trend-following trading strategy capable of exploiting linear correlations present in the S&P dataset and absent in the model. Trading signals are model-based and not derived from chartist criteria. In-sample and out-of-sample tests indicate that the model-based trading strategy performs better than a benchmark one established on an asymmetric GARCH process, and show the existence of small arbitrage opportunities. We remark that in the absence of linear correlations the trading profit would vanish and discuss why the trading strategy is potentially interesting to hedge volatility risk for S&P index-based products.

keywords: Anomalous scaling; Memory; Intraday returns; Intraday strategy.

I. INTRODUCTION

Recent studies of high frequency (HF) data for foreign exchange (FX) rates [5, 7, 22] regarded the many daily realizations of asset returns as constituting a statistical ensemble of histories¹. The single HF time series from which such ensembles can be extracted are known to present clear periodic patterns, with period of one day [see for instance 1–3, 11, 14]. For example, in the EUR/USD case, the volatility over successive 10 minutes intervals monotonically increases or decreases during specific time windows within the day. This behaviour is observed by averaging the volatility on both a daily and a weekly basis. The idea in Baldovin *et al.* [5], Bassler *et al.* [7] is to endogenize the periodic, nearly deterministic behavior of the EUR/USD exchange rate HF volatility into a time inhomogeneous stochastic process for the evolution of the asset. The analysis of the ensemble of daily histories produced by such a process reveals also a peculiar form of scaling obeyed by the probability density functions (PDF) of the returns, once they are aggregated over intervals of variable span within a fixed intraday window [see also 17]. We recall that the scaling symmetry is a relation linking the marginal PDF of a stochastic process with the duration of sampling or observation interval. In the simplest case of time intervals starting at the beginning of the daily window, the scaling property observed for EUR/USD exchange rate implies that the PDF $p(r, \tau)$ for a return r over an interval of width τ , once multiplied by a factor τ^D , yields a specific function of r/τ^D :

$$p(r, \tau) = \frac{1}{\tau^D} g\left(\frac{r}{\tau^D}\right), \quad (1)$$

where g is the scaling function, and D is a suitable scaling exponent. This form leads to $p(r/\lambda^D, \tau/\lambda) = \lambda^D p(r, \tau)$, for arbitrary rescaling λ of the interval time-span τ , and means that the PDF of the returns has a known structure, independently from the duration of aggregation intervals. A process with such a property is thus called *self-similar*. Whenever the returns of a given asset satisfy Eq. (1), a (power-law) decrease with time τ in the volatility is associated to $D < 1/2$, whereas (power-law) volatility increases are related to $D > 1/2$. However, self similarity contains more information than this. At a first level, it fixes the distribution and the behavior of all the moments of the aggregated returns, and this opens for instance the possibility of unconditioned predictions associated to the quantile function of

¹ Where a *statistical ensemble* is a collection of elements, such as a collection of realizations of a stochastic process, with given statistical properties. In the cited contributions, each daily HF dataset constitutes a single element of the ensemble. Furthermore, each element of the ensemble is assumed to be a realization of the same underlying stochastic process. The properties of the process at a given time within the day are estimated on the basis of ensemble statistics, i.e. by averaging over all available daily realizations.

these distributions. More deeply, we will see in what follows that it also permits the construction of a multivariate PDF for modeling the underlying process. This in turn enables conditioned forecasting.

The HF scaling symmetry (1) addressed in Refs. [5, 7] has specific interesting aspects: g is non-Gaussian and, for the first hours of the morning trading, D is lower than $1/2$. On the basis of the stability of the Gaussian density under time aggregation, one would expect $D = 1/2$ and a Gaussian g for independent returns. On the other hand, sliding-window empirical analysis of the returns distribution of single historical time series reveals a non-Gaussian scaling but with $D \simeq 1/2$. The deviation from Gaussianity is an anomalous scaling feature generally ascribed to long range dependence (as revealed, e.g., by the presence of volatility clustering and heteroskedasticity with persistent behaviours). However, for single time-series analysis of efficient markets historical data one still has $D \simeq 1/2$ [6, 11]. In the HF EUR/USD case mentioned above, besides non-Gaussianity the strong deviation of D from $1/2$ emphasizes the anomalous character of the scaling and implies the time-inhomogeneity (non-stationarity) of the returns' process. In particular, in Baldovin *et al.* [5] this time inhomogeneous scaling has been attributed to a non-Markovian, strong dependence of the intraday returns, as, e.g., manifested by the analysis of the ensemble-averaged volatility autocorrelation function. This strong dependence amounts to an effective volatility clustering phenomenon, partially hidden by the fact that the average 10-minutes volatility reduces in time when $D < 1/2$. By imposing consistency with the anomalous scaling of the aggregated return PDF, a martingale model has been then introduced for generating the histories in the ensemble. Within this model, the PDF of each return retains memory of the previous ones. Once properly calibrated, the model replicates very well the non-linear statistical properties of the empirical HF ensemble in the case of EUR/USD data. In particular, it is able to reproduce the patterns observed for the autocorrelations of absolute returns and squared returns obtained from the HF data.

In the present work we apply and extend the non-Markovian model introduced in Baldovin *et al.* [5] to the description of the HF data of a different financial asset, namely the S&P 500 index. A first goal is to show that the model is able to replicate the martingale morning features of an asset different from FX exchange rates. We will then extend our approach to include the description of the first part of the afternoon trading, up to 16:00 p.m., where a different, increasing, power-law behaviour of the volatility can be associated to a more complicated scaling symmetry than the one reported in Eq. (1).

In order to outline a practical application of the above stochastic modeling, we will finally devise a trading strategy built on the unconditioned and conditioned quantile functions predicted by the model. We will show that the proposed trading strategy exposes small arbitrage opportunities related to linear correlations present in the S&P dataset albeit by construction absent in our martingale model. We also compute density forecasts using a simpler and more standard GARCH martingale process [8, 12]; namely, the asymmetric GJR model [13]. The density forecasts obtained from our model and those of the GARCH benchmark are used to define price bounds whose violation gives a trading signal. The bounds might be interpreted as predicted supports and resistances, or they could be read as a simulated price range with a given confidence interval. Our trading approach is a trend following protocol which thus belongs to the large plethora of Technical Analysis-based methods whose performances have been studied by different authors [18–20, among others]. However, the indicators used here to derive the trading signals are model-based and not derived from a pure *chartist* approach. In-sample and out-of-sample tests demonstrate the existence of trading opportunities, leading, anyhow, to relatively small average margins of profit. As a matter of fact, those profits vary over time, reaching interesting values in specific periods and always beating the average profits based on the GARCH model forecasts.

The paper proceeds as follow. In subsection 1.1 we briefly describe the data used within this study, while Section 2 is devoted to the presentation of the model and to parameter calibration. Section 3 presents the version of the model suitable to describe a wider daily window of market activity. Section 4 deals with the construction of density forecasts, and Section 5 describes the trading strategy and reports the empirical results. Section 6 concludes.

A. Data extraction

In this work we focus on the S&P 500 index. We consider a dataset ranging from September 30th 1985 to October 19th 2010. After excluding those days for which the records are not complete (*e.g.*, for holidays or stock market anticipated closures), the whole dataset includes $M = 6179$ trading days. Because of dataset limitations, we exclude the first and last half an hour of each daily trading session. Such a choice has a further effect: the intra-daily periods with highest volatility, i.e. opening and closing, are excluded from the analysis. For each single day l ($1 \leq l \leq M$), in the first part of our analysis, we extract the index values, $s_t^{(l)}$, every 10 minutes between 10:00 a.m. (when we set $t = 0$) and 13:20 a.m. ($t = 20$), New York time. The reasons to choose a 10 minutes time interval will be made clearer in the following.

The empirical returns of the l -th day are thus defined as $r_t^{(l)} \equiv \ln s_t^{(l)} - \ln s_{t-1}^{(l)}$ and are regarded as specific realizations of stochastic variables R_t . Our first task is thus to identify a proper analytical model for the joint PDF of the returns

R_t , $p(r_1, r_2, \dots, r_\tau)$, which correctly reproduces the statistics of the ensemble $\left\{r_t^{(l)}\right\}_{\substack{l=1, \dots, 20 \\ t=1, \dots, M}}$. Since we will assume a martingale stochastic modeling, we checked that linear correlation effects among consecutive returns are negligible to a reasonable approximation². In Section 3 we extend the analysis up to 16:00 p.m. New York time, our ensemble hence becomes $\left\{r_t^{(l)}\right\}_{\substack{l=1, \dots, 36 \\ t=1, \dots, M}}$.

II. THE MODEL

In Bassler *et al.* [7], Seemann *et al.* [22] it has been suggested that HF financial time-series for the FX exchange rates offer the opportunity to deal with many realizations of the same stochastic process every day. The set of daily histories, restricted to suitable time-windows, can thus be regarded as an ensemble for testing the statistical properties of the underlying process. In fact these histories are not completely independent, because heteroskedasticity and volatility correlations, if estimated by time averages along the whole time series s_t from which the ensemble $s_t^{(l)}$ is extracted, exceed the intraday range. However, for a large enough total number of days M one can expect inter-day correlations effects to compensate, allowing for a reliable statistics of the postulated ensemble.

The general ideas at the basis of the mathematical model adopted here to describe such an ensemble can be traced back in Refs. [5, 6]. Financial market returns in the HF ensemble relative to the EUR/USD exchange rate are, to a first approximation, linearly uncorrelated if taken over intervals of 10 minutes or more. However, they are also dependent, as shown, e.g., by the nonzero volatility autocorrelation function. As a simplifying assumption, we also disregard the weak skewness of the returns distribution, whose inclusion in the modeling framework is left to a future development. Based on these evidences and on the existence of time inhomogeneous anomalous scaling properties (see below), it has been proposed that the joint PDF's of these returns have the form of convex combinations of the joint PDF's of processes with independent Gaussian increments of different, time dependent widths. This implies that the scaling function g of the aggregated return PDF is also a convex combination of Gaussians of variable width [21, 23], as often assumed in phenomenological studies of anomalous scaling [see, e.g., 9].

The starting point of our modeling is the assumption of the validity of the scaling symmetry, Eq. (1), for the aggregated return over the time scale τ , $\sum_{t=1}^{\tau} R_t$, with a non-Gaussian scaling function g and $D < 1/2$. This assumption is reasonably well verified in the morning window ($1 \leq \tau \leq 20$). Consistently with a power-law decay of the volatility $\sqrt{\mathbb{E}[R_t^2]}$ during the morning trading hours, an exact scaling symmetry with $D < 1/2$ also implies a power-law behavior for all the existing moments of the distribution, according to

$$\mathbb{E}[|R_1 + \dots + R_\tau|^q] = \mathbb{E}[|R_1|^q] \tau^{qD}. \quad (2)$$

The main feature of the time-inhomogeneous model described in Baldovin *et al.* [5] is the construction of the multivariate returns PDF, $p(r_1, r_2, \dots, r_\tau)$,³ on the basis of the scaling symmetry valid for the marginal PDF of the aggregated returns. Indeed, the joint PDF for the returns is reconstructed as

$$p(r_1, r_2, \dots, r_\tau) = \int_0^\infty d\sigma \rho(\sigma) \prod_{t=1}^{\tau} \frac{\exp\left(-\frac{r_t^2}{2\sigma^2 a_t^2}\right)}{\sqrt{2\pi\sigma^2 a_t^2}}, \quad (3)$$

where

$$a_t \equiv [t^{2D} - (t-1)^{2D}]^{1/2}, \quad (4)$$

$\rho(\sigma) \geq 0$ is a PDF for a mixture of Gaussian processes with different widths σ [see, e.g., 10, 25], and the scaling function g is given by

$$g(r) = \int_0^\infty \rho(\sigma) \frac{e^{-\frac{r^2}{2\sigma^2}}}{\sqrt{2\pi\sigma^2}} d\sigma. \quad (5)$$

² The mean empirical linear correlation of 10-minute returns is $\frac{1}{20} \sum_{t=1}^{20} \frac{\sum_l r_t^{(l)} r_{t+1}^{(l)}}{\sqrt{\sum_l (r_t^{(l)})^2} \sqrt{\sum_l (r_{t+1}^{(l)})^2}} \simeq 0.05$.

³ For simplifying our notations, we remove the stochastic variables subscripts to the PDF's symbols. Explicit inclusion of the arguments thus discriminates whether for instance we are talking about a single-point marginal PDF, or about a many-point joint PDF.

The coefficients a_t determine the time-inhomogeneity of the variables R_t , which is also manifest in a peculiar scaling form for its marginal PDF, $p(r_t)$. Namely,

$$p(r_t) = \frac{1}{a_t} g\left(\frac{r_t}{a_t}\right). \quad (6)$$

Only for $D = 1/2$ the variables R_t become identically distributed. See Refs. [6, 23] for additional details on the derivation of the joint PDF.

The next step is the identification of a proper parametrization for the scaling function g . As σ is a measure of volatility, many possible modelings are available in the literature [see, *e.g.*, 9, 16, 21]. A convenient way of representing fat-tailed scaling functions as those revealed by empirical analyses in finance, with the additional benefit that the integration over σ can be performed explicitly, is by using an *inverse-gamma* density for σ^2 . With this particular choice $\rho(\sigma)$ becomes

$$\rho(\sigma) = \frac{2^{1-\frac{\alpha}{2}}}{\Gamma(\frac{\alpha}{2})} \frac{\beta^\alpha}{\sigma^{\alpha+1}} e^{-\frac{\beta^2}{2\sigma^2}}, \quad (7)$$

where $\alpha > 0$ and $\beta > 0$ are a *form* and a *scale* parameter, respectively, and Γ is the Euler's gamma function. The resulting scaling function is then a Student's t-distribution,

$$g(r) = \frac{\Gamma(\frac{\alpha+1}{2})}{\sqrt{\pi} \Gamma(\frac{\alpha}{2})} \frac{1}{\beta} \left(1 + \frac{r^2}{\beta^2}\right)^{-\frac{\alpha+1}{2}}. \quad (8)$$

This $g(r)$ has a power-law decay for large $|r|$ with exponent $\alpha + 1$, whereas β simply sets the scale of its width. Moreover, with the choice in Eq. (7) for $\rho(\sigma)$, we have

$$\mathbb{E}[|R_1 + \dots + R_\tau|^q] = \frac{\Gamma\left(\frac{q+1}{2}\right) \Gamma\left(\frac{\alpha-q}{2}\right) \beta^q}{\sqrt{\pi} \Gamma\left(\frac{\alpha}{2}\right)} \tau^{qD}. \quad (9)$$

In this paper we discuss the application of this model to the S&P 500 index, working with a larger set of realizations ($M = 6179$) with respect to the EUR/USD dataset used in Baldovin *et al.* [5]. We find that the general features described in Ref. [5] also characterize the S&P 500 index within the morning time window, and that the model described above reproduces well these features. In both cases the volatility at 10 minutes intervals tends to decrease in the chosen window. In the Appendix we report additional elements about the small linear correlations of returns at the 10 minutes time-scale and the simultaneous presence of strong non-linear correlations. In the next Section we report instead the empirical evidence used to calibrate the three parameters (D, α , and β) for the morning trading session.

A. Morning calibration

The scaling exponent D and the scaling function g play here a central role as they determine respectively the a_i 's and $\rho(\sigma)$ appearing in the joint PDF [Eq. (3)] of a given daily realization of the process. We adopt a multi-step calibration procedure. At first, we calibrate D , and then we use D in order to obtain a data-collapse which allows identifying α and β [thus $\rho(\sigma)$ and g – see Eqs. (7) and (5)].

A quantitative way to calibrate D is offered by the analysis of the moments of $R_1 + \dots + R_\tau$, since in the presence of a simple scaling symmetry the moments of the aggregated returns satisfy Eq. (2), where only $\mathbb{E}[|R_1|^q]$ depends on g . The logarithm of Eq. (2) gives thus a linear relation vs q , with slope equal to D . Calling $qD(q)$ the exponent empirically estimated for the power law in Eq. (2), in Fig. 1 we plot the results of the linear regression, $qD(q) \simeq qD_m$, of the logarithm of the empirical moments as a function of τ

$$\overline{|r_1 + \dots + r_\tau|^q} \equiv \frac{1}{M} \sum_{l=1}^M |r_1^{(l)} + \dots + r_\tau^{(l)}|^q \quad (0 < q < 2). \quad (10)$$

The resulting regression slope $D(q) = D_m \simeq 0.35$, identifies the value of D for the morning trading session and is consistent with the anomalous scaling symmetry [Eq. (1)] satisfied by the empirical S&P 500 data. This value is very

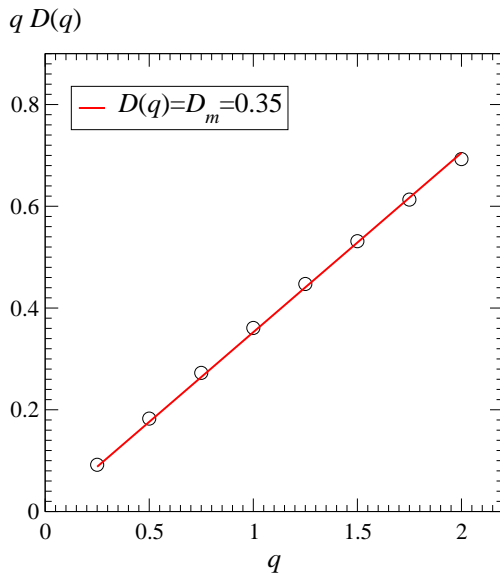


FIG. 1: Scaling behaviour of the non-linear moments.

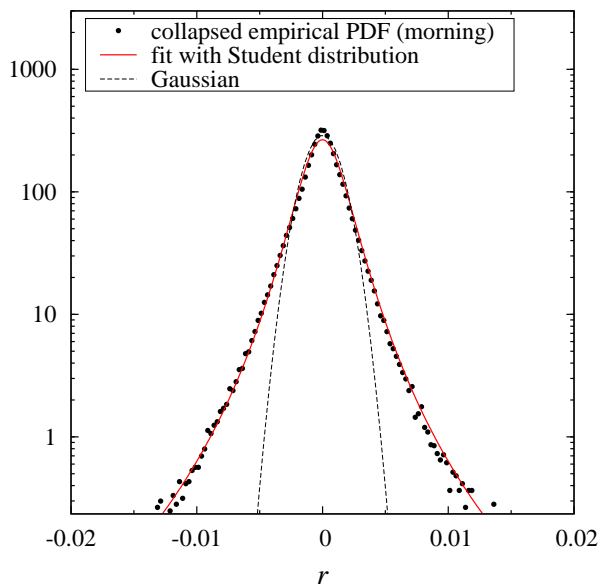


FIG. 2: The scaling function for the S&P after collapse of aggregated and marginal returns (points) in the morning time window. The red line is a fit to the points with the Student distribution given in Eq. (8).

close to that estimated for FX exchange rates in Refs. [5, 7, 22]. This is probably due to the fact that the 10-minutes volatility has a very similar decreasing trend in the window considered in the two cases. It is important to point out that we limit our scaling analysis to $q \lesssim 2$ because of an evident multiscaling behaviour for $q \gtrsim 2$ [see also 24].

Taking advantage of the knowledge of the (morning) scaling exponent $D_m = 0.35$, we now fix a relation between α and β , still analyzing the moments of the aggregated returns. Thus, a least squares fitting of $|r_1 + \dots + r_\tau|$ using Eqs. (2) with $q = 1$ and $D = D_m$ fixes $\mathbb{E}[|R_1|] \simeq 1.5 \cdot 10^{-3}$. Through Eq. (9), this gives, e.g., β as a function of α .

Finally, we data-collapse the empirical PDF of the aggregated returns $R_1 + \dots + R_\tau$ and of the marginal returns R_t , using Eq. (1) with $\tau = 1, 2, \dots, 20$ and Eq. (6) with $t = 1, 2, \dots, 20$, respectively (see Fig. 2). A least squares optimization of this data-collapse with Eq. (8) and β fixed as described above allow us to determine $\alpha \simeq 3.29$.

In summary the (in-sample) model calibration for the morning trading session gives $D = D_m = 0.35$, $\alpha = 3.29$,

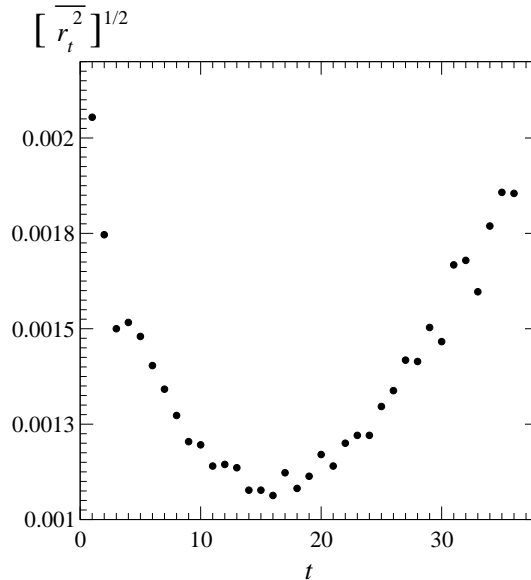


FIG. 3: Empirical volatility of the S&P dataset, during a whole trading day.

$\beta = \beta_m = 2.5 \cdot 10^{-3}$. These notations anticipate that in the extension of the model to the afternoon session we keep the form parameter α fixed, and change the value of the scaling exponent D and of the scale parameter β . As explained below, this is done consistently with the empirical analysis of the afternoon dataset.

III. EXTENSION OF THE MODEL TO THE AFTERNOON TRADING SESSION

For the purpose of extending our modeling, let us first recast Eqs. (3) and (7) by performing the transformation $\sigma \mapsto \sigma/\beta$:

$$p(r_1, r_2, \dots, r_\tau) = \int_0^\infty d\sigma \rho'(\sigma) \prod_{t=1}^\tau \frac{\exp\left(-\frac{r_t^2}{2\sigma^2 a_t^2 \beta^2}\right)}{\sqrt{2\pi\sigma^2 a_t^2 \beta^2}}, \quad (11)$$

$$\rho'(\sigma) = \frac{2^{1-\frac{\alpha}{2}}}{\Gamma(\frac{\alpha}{2})} \frac{1}{\sigma^{\alpha+1}} e^{-\frac{1}{2\sigma^2}}. \quad (12)$$

Within this formulation it is clearer the role of β as a scale parameter of the returns variables.

Fig. 3 shows that, consistently with our modeling for the morning session, during the morning hours the empirical return volatility $\sqrt{r_t^2}$ decreases. However, around $t = t^* \simeq 20$ (13:20 New York time) this trend is definitely inverted. Within our approach, an unconditioned (power-law) volatility increase can only be associated with a scaling exponent $D > 1/2$. The simplest way to extend our model is thus to keep the validity of Eq. (12) and generalize Eqs. (4) and (11) by introducing a time dependence of the scaling exponent $D \mapsto D_t$ and of the scale parameter $\beta \mapsto \beta_t$:

$$a_t \equiv [t^{2D_t} - (t-1)^{2D_t}]^{1/2}, \quad (13)$$

$$p(r_1, r_2, \dots, r_\tau) = \int_0^\infty d\sigma \rho'(\sigma) \prod_{t=1}^\tau \frac{\exp\left(-\frac{r_t^2}{2\sigma^2 a_t^2 \beta_t^2}\right)}{\sqrt{2\pi\sigma^2 a_t^2 \beta_t^2}}. \quad (14)$$

Specifically, a natural choice which leaves unchanged all the morning features and introduces the aforementioned afternoon volatility power law increase is

$$D_t \equiv \begin{cases} D_m & \text{if } 1 \leq t \leq t^* ; \\ D_a & \text{if } t^* \leq t \leq 36 , \end{cases} \quad (15)$$

$$\beta_t \equiv \begin{cases} \beta_m & \text{if } 1 \leq t \leq t^* ; \\ \beta_a & \text{if } t^* \leq t \leq 36 , \end{cases} \quad (16)$$

with $D_a > 1/2$. Explicit integration over σ leads to

$$p(r_1, \dots, r_\tau) = \left(\prod_{t=1}^{\tau} \frac{1}{a_t \beta_t} \right) \frac{\Gamma\left(\frac{\alpha+\tau}{2}\right)}{\pi^{\frac{\tau}{2}} \Gamma\left(\frac{\alpha}{2}\right)} \left[1 + \left(\frac{r_1}{a_1 \beta_1}\right)^2 + \dots + \left(\frac{r_\tau}{a_\tau \beta_\tau}\right)^2 \right]^{-\frac{\alpha+\tau}{2}} . \quad (17)$$

In the Appendix we show that this scaling-inspired, martingale extension of the model well reproduces the non-linear correlation structure of empirical returns, both during the morning and the afternoon trading sessions.

With this extension of the model, the scaling symmetry takes the form:

$$p(r, \tau) = \frac{1}{\lambda(\tau, t^*)} g' \left(\frac{r}{\lambda(\tau, t^*)} \right), \quad (18)$$

with

$$\lambda(\tau, t^*) \equiv \left(\sum_{t=1}^{\tau} a_t^2 \beta_t^2 \right)^{1/2} = \begin{cases} \beta_m \tau^{D_m} & \text{if } 1 \leq \tau \leq t^* ; \\ [\beta_m^2 (t^*)^{2D_m} + \beta_a^2 [\tau^{2D_a} - (t^*)^{2D_a}]]^{1/2} & \text{if } t^* \leq \tau \leq 36, \end{cases} \quad (19)$$

and

$$g'(r) = \frac{\Gamma\left(\frac{\alpha+1}{2}\right)}{\sqrt{\pi} \Gamma\left(\frac{\alpha}{2}\right)} (1+r^2)^{-\frac{\alpha+1}{2}} . \quad (20)$$

Clearly for $\tau \leq t^*$, Eq. (18) reduces to Eq. (1), taking into account Eq. (19) and the fact that $g(x) = \frac{1}{\beta_m} g' \left(\frac{x}{\beta_m} \right)$. In addition, the marginal single-return distribution preserves a scaling form which generalizes Eq. (6) into

$$p(r_t) = \frac{1}{a_t \beta_t} g' \left(\frac{r_t}{a_t \beta_t} \right) \quad (21)$$

with $g'(r)$ given by Eq. (20). Fig. 4 shows the consistency of these extended scaling laws with the empirical evidence. Finally, Eq. (9) for the moments of the aggregated returns distribution is now replaced by

$$\mathbb{E}[|R_1 + \dots + R_\tau|^q] = \frac{\Gamma\left(\frac{q+1}{2}\right) \Gamma\left(\frac{\alpha-q}{2}\right)}{\sqrt{\pi} \Gamma\left(\frac{\alpha}{2}\right)} [\lambda(\tau, t^*)]^q . \quad (22)$$

A. Afternoon calibration and out-of-sample calibration

While D_m , α , β_m have been (in-sample) calibrated as described in Section 2.1, D_a and β_a remain to be identified. We fix β_a by imposing a matching condition on the width of the marginal PDF $p(r_{t^*})$. Namely,

$$\beta_a = \beta_m \frac{[(t^*)^{2D_m} - (t^* - 1)^{2D_m}]^{1/2}}{[(t^*)^{2D_a} - (t^* - 1)^{2D_a}]^{1/2}} \quad (23)$$

In this way, the only parameter which remains to calibrate is D_a . Again we opt for a least squares fitting of $|r_1 + \dots + r_\tau|$ for $\tau > t^*$, using Eqs. (22) with $q = 1$. The result is $D_a \simeq 1.31$ and thus $\beta_a \simeq 7.5 \cdot 10^{-5}$. Fig. 5 displays that indeed our model well reproduces the empirical first moment of the aggregated returns, both in the morning and in the afternoon trading sessions. Summarizing our results for the in-sample calibration, we have thus $(D_m, D_a, \alpha, \beta_m, \beta_a) = (0.35, 1.31, 3.29, 2.5 \cdot 10^{-3}, 7.5 \cdot 10^{-5})$.

However, we are interested in performing out-of-sample analyses also. In such cases, starting from our 25-years database, we decided to use the first 15 years of data (from 1985 to 1999) to identify specific values for the parameters $(D_m, D_a, \alpha, \beta_m, \beta_a)$ to be used to realize the trading strategy for the year 2000. We then repeatedly shifted year by year, always using the 15 previous years to calibrate the model, until 2010. So, *e.g.*, we used the data from 1994 to 2008 to fit the scaling function for the strategy to be used for year 2009. Fig. 6 shows the optimal parameter values used for the implementation of the out-of-sample strategies from 2000 to 2010. We observe that D_a is almost stable in the out-of-sample evaluation while D_m tends to increase with time. Furthermore, the scale parameters β_m and β_a are quite stable while α decreases with time.

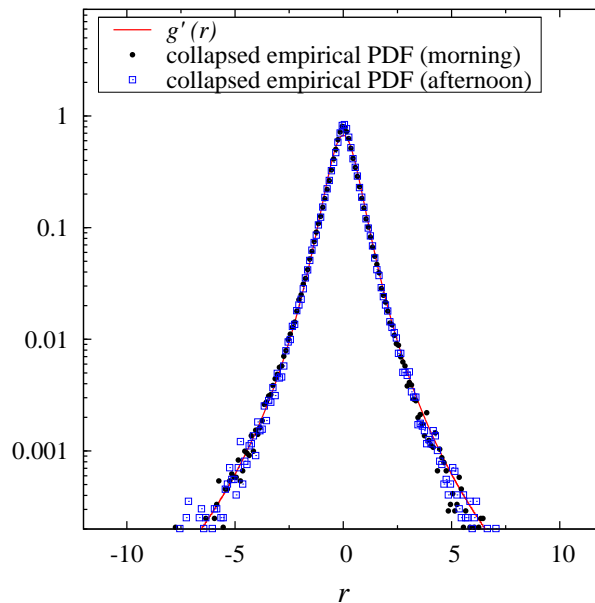


FIG. 4: The scaling function for the S&P after collapse of aggregated and marginal returns in the morning and afternoon time windows. Red line is the Student distribution given in Eq. (20) .

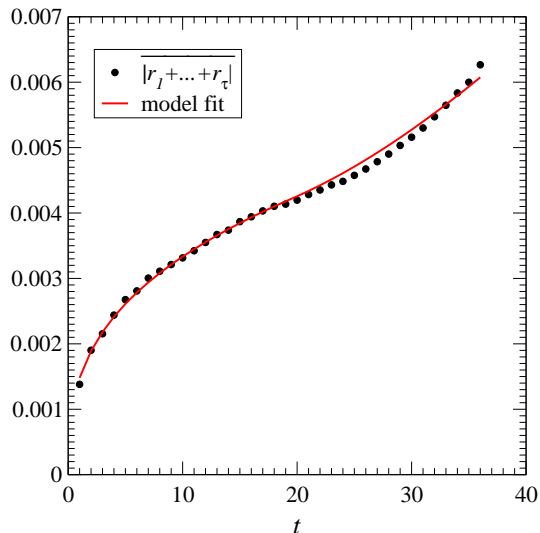


FIG. 5: Empirical first moment of the aggregated returns during a whole trading day and data fit using the model.

IV. DENSITY FORECASTS AND TRADING SIGNALS

The model proposed here is a martingale with implicit forecasting capabilities of the asset's fluctuations. Assuming correct model specifications and given the parameter values and the first t_p daily returns, the model determines, under the martingale assumption, the conditional PDF of the returns at $t > t_p$. Of course, this also gives the conditional PDF of any aggregation of subsequent returns within the validity of the extended model. Using these density forecasts it is possible to construct a trading strategy. We consider in the following two different trading approaches: the first makes use of the opening value on each day l of the traded asset at the beginning of the chosen time-window, $s_0^{(l)}$, and then bases the density forecasts only on this value. We call it *unconditioned trading* since no information coming

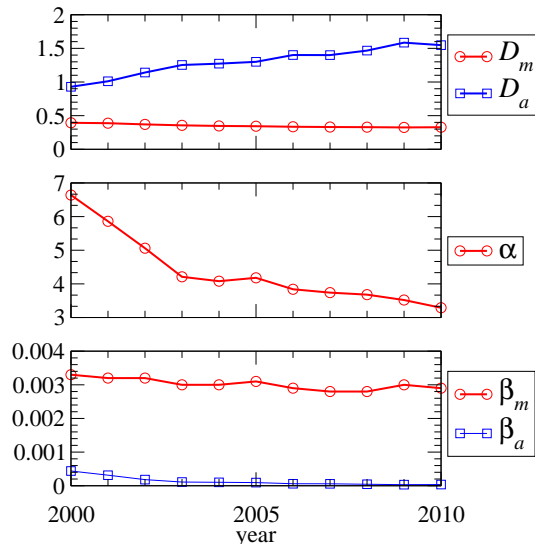


FIG. 6: Fitting parameters for the out-of-sample analysis (using 15 previous years).

from the daily returns is exploited ($t_p = 0$). In the second approach, besides $s_0^{(l)}$, we use the information contained in the first daily returns (up to $t_p > 0$) for the density forecasts of the remaining part of the daily window.

With both trading approaches it is possible to extract trading signals from density forecasts: given a certain value $0 < Q < 1/2$, if at a certain time within the intra-daily range under study the observed market price is above (below) the quantile function in $1 - Q$ (Q) of the predicted price PDF we have a buy (sell) signal. These signals are regarded as potential warnings of the presence of a trend, which, although absent in our stochastic modeling, affects the real assets' dynamics, as testified by the existence of a small, non-vanishing empirical linear correlations. Indeed, the trend-following trading strategy outlined below gives close to zero profit if applied on histories generated numerically on the basis of our martingale model.

A. Unconditioned trading signals

In this case, for each day l , we calculate the quantile function for the expected price distribution at time t , conditioned to the opening value $s_0^{(l)}$ only. Note that our approach, in computing the density forecasts, does not rely on specific previous-days information on the asset. It is assumed that all the information contained in the past observations is contained in the model parameters, namely $(D_m, D_a, \alpha, \beta_m, \beta_a)$. According to Eqs. (18) and (20), the PDF for the aggregated return $R_1 + \dots + R_\tau$ is given by:

$$p(r, \tau) = \frac{\Gamma(\frac{\alpha+1}{2})}{\sqrt{\pi} \Gamma(\frac{\alpha}{2})} \frac{1}{\lambda(\tau, t^*)} \left[1 + \left(\frac{r}{\lambda(\tau, t^*)} \right)^2 \right]^{-\frac{\alpha+1}{2}}, \quad (24)$$

with $\lambda(\tau, t^*)$ as in Eq. (19). The lower-bound values $r_{min, \tau}(Q)$ of the expected aggregated returns for the value Q of the cumulative distribution are then obtained by numerically solving the equation

$$Q = \int_{-\infty}^{r_{min, \tau}(Q)} dr p(r, \tau) \quad (25)$$

with respect to $r_{min, \tau}(Q)$. Due to the parity of the scaling function $g(r)$, the corresponding upper-bound values $r_{max, \tau}(Q)$ are simply obtained via sign flip: $r_{max, \tau}(Q) = -r_{min, \tau}(Q)$.

The lower and upper expected values, $s_{min, \tau}(Q)$ and $s_{max, \tau}(Q)$, respectively, of the asset price at time τ can then be easily calculated. Indeed, given $s_0^{(l)}$, the asset price S_τ is a monotonic function of the R_t 's:

$$S_\tau = s_0^{(l)} e^{\sum_{t=1}^{\tau} R_t}. \quad (26)$$

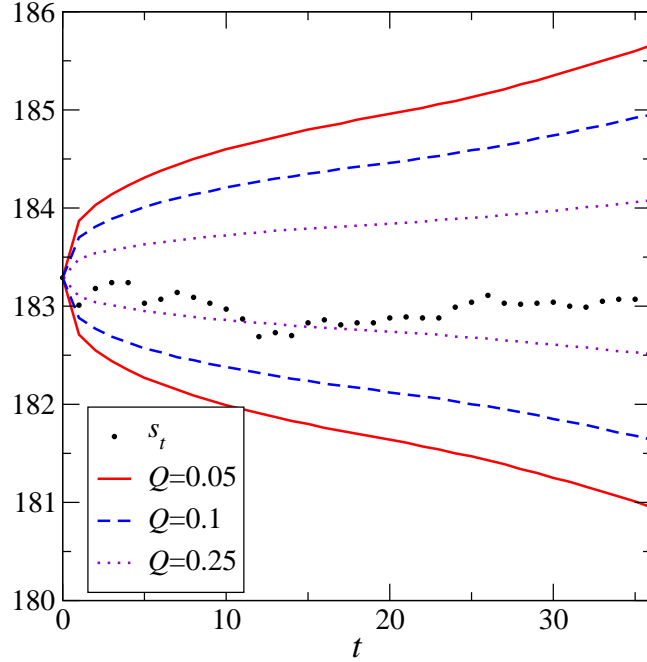


FIG. 7: Upper and lower expected index values for October 4th 1985, confronted with real prices (black circles). Lines are linear piece-wise interpolations.

Hence, the quantile function for S_τ is directly related to those of R_t 's, once the daily opening value is given. Notice that in order to simplify our notations, we have dropped the dependence of $s_{min,\tau}(Q)$ and $s_{max,\tau}(Q)$ on the trading day.

Summarizing, for every choice of Q with $0 < Q < 1/2$, for every time t from 1 to 36 within each trading day, two price barriers are obtained, $s_{min,\tau}(Q)$ and $s_{max,\tau}(Q)$. According to our martingale modeling, with probability $1 - 2Q$ the price at time t is placed between these barriers. For instance, in Fig. 7 the results of the in-sample analysis for the day October 4th, 1985, are shown. As detailed below, the comparison between these barrier values and the actual real market price lead us to the definition of a buy or sell action which will be shown to be able of exploiting trends present in the real data.

The empirical analysis considers both in-sample and out-of-sample cases. The difference between the two is that for the former a unique set of values $(D_m, D_a, \alpha, \beta_m, \beta_a)$ is used, calibrated with the whole 25-year dataset, while in the latter case the parameters $(D_m, D_a, \alpha, \beta_m, \beta_a)$ are calibrated each year, on the basis of the previous 15-year history. For both approaches we will use the cumulative distribution values $Q = 0.05, 0.1, 0.25$ (5%, 10%, 25%, respectively).

B. Conditioned trading signals

To exploit the non-Markovian character of our model, besides the opening value of the day, $s_0^{(l)}$, we can use the value of the first t_p returns of the day, r_1, \dots, r_{t_p} ,⁴ to condition the subsequent expected evolution of the index.

In general, the conditioned probability of the aggregated returns $r_{t_p+1} + \dots + r_{t_p+\tau}$ given the previous ones r_1, \dots, r_{t_p} is obtained as the ratio of the joint PDF's:

$$p(r, \tau | r_1, \dots, r_{t_p}) = \frac{p(r, \tau; r_1, \dots, r_{t_p})}{p(r_1, \dots, r_{t_p})}. \quad (27)$$

⁴ Again, for simplicity dependence on the day l is understood.

Using Eq. (17), we obtain the explicit expression

$$p(r, \tau | r_1, \dots, r_{t_p}) = \frac{\Gamma\left(\frac{\alpha+t_p+1}{2}\right)}{\pi^{\frac{1}{2}} \Gamma\left(\frac{\alpha+t_p}{2}\right)} \left(\sum_{t=t_p+1}^{t_p+\tau} a_t^2 \beta_t^2 \right)^{-1/2} \cdot \frac{\left[1 + \frac{r^2}{\sum_{t=t_p+1}^{t_p+\tau} a_t^2 \beta_t^2} + \left(\frac{r_1}{a_1 \beta_1}\right)^2 + \dots + \left(\frac{r_\tau}{a_\tau \beta_\tau}\right)^2 \right]^{-\frac{\alpha+t_p+1}{2}}}{\left[1 + \left(\frac{r_1}{a_1 \beta_1}\right)^2 + \dots + \left(\frac{r_{t_p}}{a_{t_p} \beta_{t_p}}\right)^2 \right]^{-\frac{\alpha+t_p}{2}}}. \quad (28)$$

In this way, with a simple change of variable the equation defining the conditioned quantile function,

$$Q = \int_{-\infty}^{r_{min,\tau}(Q)} dr p(r, \tau | r_1, \dots, r_{t_p}), \quad (29)$$

becomes

$$Q = \frac{\Gamma\left(\frac{\alpha+t_p+1}{2}\right)}{\pi^{\frac{1}{2}} \Gamma\left(\frac{\alpha+t_p}{2}\right)} \int_{-\infty}^{z_{min,\tau}(Q)} dz [1+z^2]^{-\frac{\alpha+t_p+1}{2}}, \quad (30)$$

with

$$z_{min,\tau}(Q) \equiv \frac{r_{min,\tau}(Q)}{\left(\sum_{t=t_p+1}^{t_p+\tau} a_t^2 \beta_t^2 \right)^{1/2} \left[1 + \left(\frac{r_1}{a_1 \beta_1}\right)^2 + \dots + \left(\frac{r_{t_p}}{a_{t_p} \beta_{t_p}}\right)^2 \right]^{\frac{1}{2}}}. \quad (31)$$

Given the previous returns r_1, \dots, r_{t_p} , again Eq. (30) can be solved numerically for $r_{min,\tau}(Q)$. Knowing $s_0^{(l)}$ the determination of the conditioned lower and upper barriers, $s_{min,\tau}(Q)$ and $s_{max,\tau}(Q)$ respectively, proceeds then as indicated in the previous section.

In Fig. 8 some interesting features of conditioned trading signals can be detected. In particular, it is clear the influence of the past returns to determine the expected amplitude of the next ones. Conditioned trading will thus be based on bounds which may vary according to the information contained in the first returns of the day.

V. DEVELOPING AND APPLYING INTRADAY STRATEGIES

When the index value $s_t^{(l)}$ breaks through the lower $s_{min,\tau}(Q)$ or the upper $s_{max,\tau}(Q)$ values of the quantile function, this violation can be used to define a trading strategy. Note that the ensemble property we consider lasts from 10:00 a.m. to 16:00 p.m. As a consequence, we define a trading strategy which operates within this time lapse. To avoid the impact of news arrivals in the close-to-open time frame, the trading strategy opens and closes positions within the day. Furthermore, since we are using a 10-minute dataset, density forecasts (and therefore the quantile functions at level Q and $1-Q$) will be available from 10:00 a.m. + $(t_p+1) \times 10$ min.

Within a certain day l , given the specific values of the quantile function at level Q and $1-Q$, $s_{min,\tau}(Q)$ and $s_{max,\tau}(Q)$ respectively, the trading signals and the trading activity are defined as follows:

A: If there are no open positions

A.i: Buy if $s_t^{(l)} > s_{max,t}(Q)$ & $s_{t-1}^{(l)} < s_{max,t-1}(Q)$

A.ii: Sell if $s_t^{(l)} < s_{min,t}(Q)$ & $s_{t-1}^{(l)} > s_{min,t-1}(Q)$

B: If there are open positions

B.i: Close a long position if $s_t^{(l)} < s_{max,t}(Q)$ & $s_{t-1}^{(l)} > s_{max,t-1}(Q)$

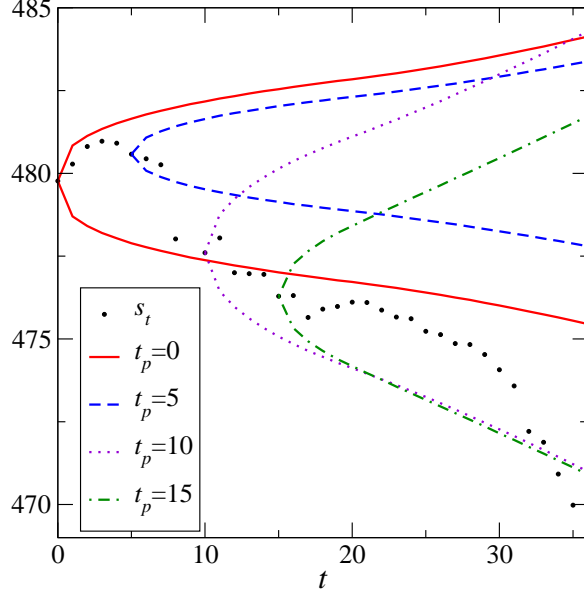


FIG. 8: Upper and lower expected index values [$Q=10\%$] for one random day of the dataset (February 4th, 1994). As shown in the inset, different numbers of conditioning returns are considered.

B.ii: Close a short position if $s_t^{(l)} > s_{min,t}(Q)$ & $s_{t-1}^{(l)} < s_{min,t-1}(Q)$

B.iii: Close long or short positions if they are still in place at market closing.

By construction, multiple trades are possible within volatile days. Differently, in trending days, single operations will take place, while during stable days, no positions will be taken.

The quantile functions built with our model assume the absence of linear correlations and then, if positive linear correlations exist, on average, an open trade will last more than expected and the probability of a positive profit will be slightly greater than the probability of a negative profit. In the light of these considerations and of our model assumptions, the choice of the 10-minutes time interval can be now better explained. Indeed, it is a compromise between the need of a fine definition of the price trajectory (for an efficient application of the strategy) and the need of having small enough linear correlations notwithstanding the presence of non-linear correlations (for a good accordance with the characteristics of the model). Furthermore, we noticed that considering a one-minute time intervals results in poorer performances of the trading strategy, likely because with such a short intervals the trades have a shorter life and thus smaller average profit.

Our purpose is to monitor the performances of the trading strategy defined above. Therefore, we simulate the time evolution of a trader using our strategy and having an initial cash amount equal to 1 million. Given the previous remarks about the validity of the ensemble properties and their link with the trading strategy, at the beginning of the day and at market closing the simulated portfolio is entirely composed by cash. Furthermore, in order to avoid losses larger than the portfolio value when implementing short positions, we limit the investment value to 90% of the overall portfolio value⁵. For symmetry, we apply the same rule also for long positions. As a result, when trades are created, 10% of the portfolio remains in cash. Once a signal is observed, the trade is executed at the price $s_t^{(l)}$.

As mentioned above, three different quantile levels will be considered: 5%, 10%, 25%, and we simulate both unconditioned and conditioned quantiles for all these three levels. Specifically, we calculate price barriers using the

⁵ We do not take into account the margins generally required when creating short position. We motivate this choice by the need of evaluating the strategy abilities on both long and short trades without penalizing short positions, as would be the case when margins larger than 10% would be required. Furthermore, given that the trades will last at maximum for 5 hours and 50 minutes (from 10:10 to 16:00 p.m.), we believe that an implicit margin of 10% will be sufficient.

TABLE I: Average profit per trade in basis points (1985-2010).

	25%	10%	5%
All trades			
0	4.479	3.473	2.722
3	4.862	4.501	3.716
6	4.525	4.285	4.166
9	4.200	4.608	3.862
Long trades			
0	4.519	3.551	4.587
3	4.886	4.775	4.119
6	4.430	4.391	4.561
9	4.354	4.830	4.514
Short trades			
0	4.441	3.403	1.283
3	4.838	4.234	3.347
6	4.625	4.185	3.833
9	4.039	4.395	3.280

The first column reports the conditioning elements (0 stands for no conditioning). The first row shows the quantile level.

opening price only (unconditioned, $t_p = 0$), or conditioning also on the first 3, 6 or 9 returns ($t_p = 3, 6, 9$, respectively). Higher numbers of initial conditioning points are not used for two main reasons: first, their introduction results in poorer performances compared to those observed with up to 9 conditioning points; second, the number of observations within the day is limited to 36 and we prefer not to reduce too much the time frame available for trading activity.

A. In-sample results

We first analyse the trading strategy in-sample, in order to evaluate its abilities in terms of yearly profits and average return by trade (in basis points). At this stage, we also verify the impact of the different number of conditioning returns. Table (I) reports the average return of the trades generated by the strategy during the period from October 1985 to October 2010. Profits are indicated as average basis points per trade, and distinguishing also between long and short trades. This allows to verify if the strategy better identifies signals in a specific direction.

Two elements clearly appear. The first one is that the profit decreases with decreasing quantile values, as if stronger signals provide smaller performances irrespective of the trade sign. We explain such an unexpected result by the fact that the linear correlations are so small that the effectiveness of the trading strategy is decreased when the quantile barriers become steeper.

The second relevant comment refers to the relation between average profit and conditioning information. We observe that conditioning the price barriers to the first returns of the day increases the profit. This is somewhat expected as during the first part of the day the model adapts its behaviour to the most recent data, and it provides therefore a better fit to the ensemble property within the remaining part of the day. Again, such a result holds independently of the trade sign. Regarding the number of conditioning values, we note that the relation between conditioning points and profits is not monotonic, and has a maximum between one and six conditioning points. As a consequence of this result and of the previous one about the quantile/profit relation, the out-of-sample analyses discussed in the next section have been performed with three conditioning points, which is the value with maximum profit for the 5% and 25% quantiles. Table (I) reports just the average trade returns. However, we also analysed the distribution and the moments of the trade returns. The results (not reported and available upon request) show that the distribution of trade returns is highly leptokurtic and right skewed (asymmetry is positive and, on average, larger than 3).

Table (II) reports the same quantities as Table (I), but by year (we drop 1985 and 2010 where only part of the year was available). In general, the use of a 25% quantile provides the higher average profit. Furthermore, we observe that the various trading strategies are concordant in showing negative values in the range 2004-2007, where the market was clearly upward trending and in a low volatility phase. This is an expected outcome, since the model detects violations which are associated with high price fluctuations. The largest profits are located during 1986 and 1987, in a high volatility period. Overall, the average profit per trade is relatively small, and occasionally even negative. On

TABLE II: Average profit per trade in basis points (yearly values).

Year Quantile	Unconditioned			Conditioned 3 points			Conditioned 6 points		
	25%	10%	5%	25%	10%	5%	25%	10%	5%
1986	11.41	11.14	7.88	12.04	13.13	11.85	11.84	10.96	11.19
1987	13.37	15.75	14.94	14.99	18.97	16.35	13.79	18.68	19.57
1988	8.94	10.02	8.74	11.16	12.44	15.50	8.73	12.46	11.55
1989	7.21	7.33	4.82	7.33	7.77	5.85	9.53	8.75	7.33
1990	8.78	5.42	3.33	9.73	6.40	5.20	9.68	6.39	4.82
1991	7.45	5.39	8.26	8.64	8.92	6.28	9.16	10.73	10.10
1992	4.36	1.97	-1.72	4.50	5.38	4.34	5.59	4.68	5.99
1993	3.11	-0.05	-0.49	3.07	3.76	1.01	2.20	2.98	3.99
1994	4.06	2.90	-2.52	4.57	3.83	1.35	4.12	4.49	4.07
1995	3.11	-0.01	1.73	3.05	2.58	1.92	2.67	3.08	0.65
1996	2.28	-0.22	-4.56	3.07	-0.50	-4.21	3.91	3.54	1.75
1997	4.3	1.83	-1.06	5.41	3.99	2.83	7.04	5.36	2.20
1998	6.15	6.42	5.39	5.90	6.43	2.76	4.90	3.30	3.05
1999	2.27	1.39	-2.70	3.07	3.29	1.11	2.58	1.28	0.00
2000	3.33	0.91	1.87	2.53	4.08	2.94	2.50	2.33	1.09
2001	1.04	1.25	0.65	1.40	0.91	2.95	2.32	0.30	-0.49
2002	7.50	6.94	7.94	5.30	3.14	5.73	3.97	0.93	1.79
2003	2.04	1.56	1.59	3.64	2.77	1.29	2.18	1.90	2.76
2004	1.27	2.98	3.08	1.01	1.48	2.20	1.40	3.21	2.97
2005	1.85	2.18	1.15	2.47	1.08	-1.00	3.13	2.43	4.26
2006	0.75	-1.85	-5.16	0.56	0.48	-1.32	0.53	0.47	-0.14
2007	-0.49	-2.07	-2.40	0.96	1.60	1.12	0.48	1.49	-1.18
2008	8.24	3.70	4.08	7.18	2.49	0.01	5.64	2.26	2.34
2009	1.82	1.87	0.49	3.91	0.62	-0.01	0.89	-1.57	-0.24

the other hand, during some specific market phases the trading strategy provides large average profits per trade, see for instance the 90's.

Besides the impact of quantile level and number of conditioning returns, a third element is of interest: the number and type of trades created by the strategy in a given time interval. Table (III) reports several elements for the most recent years. The first column just repeats the content of Table (II), while the following ones separately consider Long and Short trades distinguishing between "true" and "false" signals. We call "true" a trading signal which really provides a positive trade profit. As previously mentioned, the existence of "false" signals is also influenced by the discreteness of our dataset and the ratio true-to-false signals might not be optimal.

In light of this comment, the presence of substantial positive profits despite the relatively small number of true signals [see the last two columns of Table (III)] should be considered as a positive, potentially interesting outcome of the strategy. A further element supporting the strategy is the average profit of trades originated by true signals. Both for long and short trades, these average profits are sensibly larger, peaking at more than 150 basis points (note that trades are created within the day). On the contrary, false signals lead to trades with small losses (compared to the gains), even if these losses are larger during volatile market phases as in 2008 and 2009 (both for long and short trades). The number of trades is much larger when using 25% quantiles compared to 5% quantiles; while there are small differences between the use of Conditioned and Unconditioned quantiles. Long and short trades are almost numerically equivalent both in trending and volatile market phases. As naturally expected, the number of trades increases during volatile periods, irrespectively of the sign. Finally, also the number of relatively few true signals does not depend on the trade sign. In summary, Table (III) shows evidence of some potential interest in the proposed strategy, since the average profit for true signals is quite elevate (in particular compared to the overall average profit).

While the previous tables where focusing on the average return over single trades, Table (IV) focuses on the overall profit of the strategy over single years (assuming a starting cash amount of 1 million). The returns are reported in percentages, and show evidence of positive performances in most periods. Comparing first the Conditioned versus Unconditioned quantiles, we observe that conditioned modeling is clearly better: the associated returns are higher

TABLE III: Average profit per trade and number of trades: long/short trades, false/true signals.

	Average profit (bp)						Number of trades						% True			
	All		Long		Short		All		Long		Short		Long	Short		
	All	True	False	All	True	False	All	True	False	All	True	False				
25% - Conditioned 3 points																
2005	2.47	2.93	38.72	-5.89	2.08	41.67	-6.71	561	258	51	207	303	55	248	19.8%	18.2%
2006	0.56	1.11	32.74	-5.50	0.07	36.63	-6.55	566	266	46	220	300	46	254	17.3%	15.3%
2007	0.96	-1.30	39.94	-8.87	3.56	68.78	-9.38	650	348	54	294	302	50	252	15.5%	16.6%
2008	7.18	3.45	115.48	-22.12	10.50	141.75	-20.61	720	339	63	276	381	73	308	18.6%	19.2%
2009	3.91	2.79	83.36	-13.69	5.40	94.67	-15.54	650	371	63	308	279	53	226	17.0%	19.0%
5% - Conditioned 3 points																
2005	-1.00	0.15	30.20	-3.10	-2.30	21.54	-7.55	154	82	8	74	72	13	59	9.8%	18.1%
2006	-1.32	0.45	32.27	-3.09	-2.57	43.33	-6.05	121	50	5	45	71	5	66	10.0%	7.0%
2007	1.12	1.73	53.31	-7.32	0.78	52.20	-8.03	190	67	10	57	123	18	105	14.9%	14.6%
2008	0.01	-2.82	122.92	-17.98	2.26	127.03	-20.63	358	158	17	141	200	31	169	10.8%	15.5%
2009	-0.01	0.71	90.40	-11.25	-0.65	107.26	-12.46	288	136	16	120	152	15	137	11.8%	9.9%
25% - Unconditioned																
2005	1.85	1.53	41.88	-6.65	2.12	42.9	-6.27	542	249	42	207	293	50	243	16.9%	17.1%
2006	0.75	0.05	34.58	-6.31	1.42	42.82	-7.38	489	238	37	201	251	44	207	15.5%	17.5%
2007	-0.49	-2.19	39.94	-9.33	1.5	78.14	-11.57	654	352	51	301	302	44	258	14.5%	14.6%
2008	8.24	5.1	127.17	-28.45	11.38	156.4	-26.54	771	385	83	302	386	80	306	21.6%	20.7%
2009	1.82	2.86	92.27	-19.27	0.66	97.78	-20.65	717	378	75	303	339	61	278	19.8%	18.0%
5% - Unconditioned																
2005	1.15	5.71	66.1	-0.22	-1.34	7.07	-2.67	34	12	1	11	22	3	19	8.3%	13.6%
2006	-5.16	-1.94	4.28	-2.56	-6.93	11.43	-7.90	62	22	2	20	40	2	38	9.1%	5.0%
2007	-2.40	-0.02	67.11	-12.01	-3.38	68.96	-14.74	114	33	5	28	81	11	70	15.2%	13.6%
2008	4.08	3.31	161.15	-29.28	4.78	147.73	-27.07	469	222	38	184	247	45	202	17.1%	18.2%
2009	0.49	2.25	118.14	-16.59	-1.10	103.59	-14.87	408	193	27	166	215	25	190	14.0%	11.6%

apart from few cases, and their standard deviation is in most cases smaller⁶. Contrasting the 25% and 5% quantiles, the use of narrower bands (25%) for the identification of the signals provide larger returns over the years. This potentially exposes the portfolio to a number of trades generated by false signals, but the profits coming from true signals balance them. Such a result holds irrespectively of the conditioning type. Finally, if we compare the performances of the trading strategy (25% quantiles) to that of the underlying equity index [see the last two columns of Table (IV)], we note a relevant positive result: when the market is experiencing high volatility, our strategy provides positive returns with a volatility smaller than that of the market, and this is particularly evident when the market has yearly negative returns; on the contrary, when the market is in a low volatility period, our strategy has in some cases small or negative returns. In general, the trading strategy has always a volatility smaller than that of the market. This finding suggests that it could be used to hedge the market volatility, since it provides positive returns in case of high market volatility, and with smaller risk. This is further confirmed by the correlation between market and our strategy returns and between market and our strategy standard deviation [see the last row of Table (IV)]: positive and very high correlation in the case of standard deviations, and low negative correlation for returns. Finally, if we compute the yearly Sharpe ratios (not reported) we can note that the strategies based on 25% quantiles provide higher remuneration per unit of risk compared to the market.

⁶ The standard deviation is computed over the daily returns of the simulated portfolio and then annualized. Note that days without any trading signal provide zero returns, since we did not assume any remuneration for the bank account.

TABLE IV: In-sample yearly return and standard deviation compared with the S&P500 Index.

	25% - C. 3 p.		5% - C. 3 p.		25% - Unc.		5% - Unc.		S&P500	
	Return	Dev.st	Return	Dev.st	Return	Dev.st	Return	Dev.st	Return	Dev.st
1986	70.15	7.91	23.00	5.60	63.61	7.76	6.66	4.02	14.62	14.64
1987	89.63	15.18	38.62	11.32	79.65	18.03	23.56	16.22	2.03	32.01
1988	64.62	9.48	29.69	6.52	49.62	9.94	10.58	6.69	12.40	17.02
1989	38.48	7.59	8.55	5.90	32.48	7.26	2.81	5.73	27.25	13.01
1990	60.70	8.19	14.07	5.19	51.33	8.38	5.66	4.70	-6.56	15.89
1991	51.30	7.33	14.55	4.53	38.56	7.38	8.73	3.92	26.31	14.24
1992	22.19	4.45	5.06	2.07	17.73	4.09	-0.96	1.26	4.46	9.64
1993	14.33	3.97	1.14	1.92	10.53	3.66	-0.12	1.33	7.06	8.57
1994	22.82	4.62	1.57	2.49	16.95	4.79	-1.13	1.34	-1.54	9.80
1995	14.93	3.68	1.76	2.10	12.24	3.90	0.49	1.54	34.11	7.78
1996	16.91	5.36	-5.55	2.19	12.17	5.77	-3.46	2.78	20.26	11.73
1997	35.58	9.32	5.81	6.15	29.74	9.88	-2.50	6.15	31.01	18.06
1998	38.57	9.56	6.20	4.78	40.12	11.47	11.98	7.42	26.67	20.21
1999	20.60	7.66	2.89	4.03	14.68	9.79	-6.62	4.93	19.53	18.00
2000	16.06	10.46	6.88	6.18	24.10	13.02	5.62	8.80	-10.14	22.13
2001	9.15	10.32	6.20	5.26	6.30	11.96	2.36	7.04	-13.04	21.47
2002	39.53	12.82	15.27	8.99	61.15	16.42	33.80	12.86	-23.37	25.93
2003	24.70	7.92	2.27	3.84	12.71	9.53	3.82	5.11	26.38	17.00
2004	5.64	6.06	3.26	2.81	6.42	6.09	2.13	1.71	8.99	11.05
2005	13.81	4.58	-1.41	1.85	9.57	4.55	0.40	1.42	3.00	10.24
2006	2.98	4.41	-1.45	1.88	3.12	4.77	-2.89	0.91	13.62	9.99
2007	4.61	7.46	1.86	3.60	-4.31	7.92	-2.59	3.57	3.53	15.93
2008	53.19	19.62	-2.24	13.19	68.93	23.97	14.81	20.24	-38.49	40.81
2009	25.01	12.56	-0.46	7.24	11.18	15.49	1.16	10.84	24.71	27.18
Corr.	-0.10	0.99	-0.06	0.94	-0.33	0.99	-0.46	0.98		

B. Out-of-sample results

The above promising in-sample performances are confirmed in the out-of-sample results. In this evaluation, we compare our model to a more traditional approach, based on GARCH processes [8, 12]. Shifting from the point of view of ensembles to that of financial time series, several elements characterizing high frequency data have to be considered. In particular, the periodic behaviour of the intra-daily volatility has to be taken into account [3, 4, among others]. To capture these elements, together with variance asymmetry, we consider as a competing model an asymmetric GARCH, the GJR [13] with a periodic deterministic variance component. Our choice is motivated by the relative simplicity of the competitor, a kind of benchmark, and by the possibility of easily generating from this model density forecasts at a given quantile under a distributional assumption for the model innovations. The competing model is given as follow:

- the empirical returns on a 10-minute time scale are represented as: $r_t^{(l)} = m_t^{(l)} \epsilon_t^{(l)}$, where t identifies the 10-minute period within day l with a range which is now $t = 1, 2, \dots, T$ ($T = 36$ for our dataset), $m_t^{(l)}$ is a deterministic periodic function, and $\epsilon_t^{(l)}$ is the stochastic component; this model implies that returns are generated as $R_t^{(l)} = \mathbb{N}(0, m_t^{(l)} \mathbb{V}_\epsilon)$, where $\mathbb{N}(\mu, \sigma)$ indicates a Gaussian random variable of mean μ and variance σ , and \mathbb{V}_ϵ is the (stochastic) variance of the random component;
- $m_t^{(l)}$ is a periodic deterministic variance modeled similarly to Andersen and Bollerslev [4], but using dummy variables instead of harmonics; we might represent returns as

$$\ln[(R_t^{(l)})^2] = \ln[(m_t^{(l)})^2] + \ln[(\epsilon_t^{(l)})^2], \quad (32)$$

with

$$\ln[(m_t^{(l)})^2] = a_1 + \sum_{j=2}^T a_j d_{t,j}^{(l)}, \quad (33)$$

where $d_{t,j}^{(l)}$, $j = 2, \dots, T$ is a dummy variable assuming value 1 when $j = t$ and zero otherwise, while $a_1, a_2 \dots a_T$ are parameters to be estimated;

- furthermore, the stochastic term $\varepsilon_t^{(l)}$ follows a GJR model (Glosten et al. 1993) allowing thus for the decomposition

$$\varepsilon_t^{(l)} = \sigma_t^{(l)} Z_t^{(l)}, \quad (34)$$

where $Z_t^{(l)} = \mathcal{N}(0, 1)$ and the conditioned variance is given by

$$(\sigma_t^{(l)})^2 = \omega + \left(\alpha_0 + \alpha_1 I(\bar{\varepsilon}_t^{(l)} < 0) \right) (\bar{\varepsilon}_t^{(l)})^2 + \beta (\bar{\sigma}_t^{(l)})^2, \quad (35)$$

where

- $(\bar{\varepsilon}_t^{(l)})^2 \equiv (\varepsilon_{t-1}^{(l)})^2$ if $t > 1$ and $(\bar{\varepsilon}_t^{(l)})^2 \equiv (\varepsilon_T^{(l-1)})^2$ if $t = 1$,
- $(\bar{\sigma}_t^{(l)})^2 \equiv (\sigma_{t-1}^{(l)})^2$ if $t > 1$ and $(\bar{\sigma}_t^{(l)})^2 \equiv (\sigma_T^{(l-1)})^2$ if $t = 1$,
- $I(\bar{\varepsilon}_t^{(l)} < 0)$ is equal to one when $\bar{\varepsilon}_t^{(l)}$ is negative and zero otherwise,
- $\omega, \alpha_0, \alpha_1$ and β are parameters to be estimated. These parameters must satisfy the constraints for variance positivity and covariance stationarity $\omega > 0, \alpha_0 > 0, \alpha_1 > 0, \beta > 0$ and $\alpha_0 + 0.5\alpha_1 + \beta < 1$ (under an assumption of symmetry for the density characterizing $Z_t^{(l)}$).

The estimation of the model proceeds by steps. At first the periodic component is estimated by linear regression using equations (32) and (33). The fitted periodic component is used to recover the estimated values of $\epsilon_t^{(l)}$. Over those, the GJR parameters are estimated by Quasi Maximum Likelihood approaches using a Gaussian likelihood. Given the estimated parameters, and under a Gaussian density for the innovations $z_t^{(l)}$, we generate possible paths for the future evolution of the conditioned variance $(\sigma_t^{(l)})^2$, of the innovations $\epsilon_t^{(l)}$, and of the returns $r_t^{(l)}$ (the periodic component $m_t^{(l)}$ is purely deterministic and is thus simply replicated in the forecasting exercise). Under the distributional hypothesis, the needed quantiles are then determined and used as an alternative input for the identification of the trading signals.

In Table (V) we report the out-of-sample average profit per trade, using the Unconditioned and Conditioned trading strategies as well as the one based on the GJR model. As mentioned earlier, the out-of-sample evaluation focuses only in the range 2000 to 2010, since the period 1985-1999 is used to calibrate the models. Results for our model are similar to in-sample outcomes, with conditioned modeling providing better results. Both Conditioned and Unconditioned model specifications have performances largely better than the GJR model. The only case in which the conditioned variance model have performances comparable to our approach is over long trades and for quantiles equal to 25% and 10%. Even in the out-of-sample case we analyse the trade returns distribution, in particular contrasting our model's results to the GJR returns. We note that the returns distribution from the GJR model is characterised by smaller levels of both kurtosis and skewness compared to our model's results. We note that also the GJR returns distribution is right skewed (results are available upon requests).

The differences among the strategies appear more clearly in Table (VI), which contains annual returns of the simulated portfolios. We note here that using the 25% quantiles together with a conditioning on the first three returns of the day provides the best results in high volatility market phases (large than 20% annualized daily market volatility). On the contrary, when the volatility is lower, there is not a clear preference across the models (GJR included). The yearly volatility of the GJR is lower compared to our models as well as to the market, but the yearly profits are clearly unsatisfactory. In addition, the last row of Table (VI) reports the correlations between market and strategies returns and between market and strategies standard deviations: results confirm the previous in-sample findings for our strategies, while for the GJR we have a lower correlation in the standard deviations and a positive correlation between the strategy returns and the market returns.

Overall, the results suggest the existence of some trading opportunities with respect to the time series and sample size used. Furthermore, they show how the combination of advanced statistical methodologies could be used for the development of trading rules or trading schemes which have a large resemblance with those commonly used in technical analysis.

TABLE V: Out-of-sample average profit per trade in basis points (2000-2010).

	25%	10%	5%
All trades			
Unc.	2.865	2.249	1.992
Cond. (3)	2.830	1.758	1.383
GJR	0.286	0.397	0.569
Long trades			
Unc.	2.226	2.601	3.921
Cond. (3)	2.444	1.514	1.870
GJR	2.512	2.576	0.855
Short trades			
Unc.	3.488	1.950	0.459
Cond. (3)	3.203	1.990	0.965
GJR	-1.313	-1.404	0.320

The first column reports the model: Unc. stands for our model with no conditioning; Cond. (3) refers to the model with a conditioning to the first three returns of the day; finally, GARCH identifies the conditioned variance specification with deterministic periodic component. The first rows reports the quantile level.

TABLE VI: Out-of-sample yearly return and standard deviation compared with the S&P500 Index.

	25% - C. 3 p.		5% - C. 3 p.		25% - Unc.		5% - Unc.		25% - GJR		5% - GJR		S&P500	
	Return	Dev.st	Return	Dev.st	Return	Dev.st	Return	Dev.st	Return	Dev.st	Return	Dev.st	Return	Dev.st
2000	18.39	10.74	8.52	6.56	22.12	13.18	3.45	9.82	-2.04	5.12	0.19	1.60	-10.14	22.13
2001	7.65	10.39	6.11	5.48	6.48	12.01	2.60	8.13	7.18	5.20	-2.53	1.83	-13.04	21.47
2002	41.00	12.77	13.40	9.48	57.78	16.51	30.32	13.22	-5.06	5.58	-0.02	1.88	-23.37	25.93
2003	27.72	7.92	1.26	3.87	16.15	9.26	5.34	5.18	4.20	4.69	0.87	2.08	26.38	17.00
2004	5.30	5.99	3.55	2.67	6.28	5.98	1.99	1.79	-1.31	1.80	0.24	0.35	8.99	11.05
2005	13.40	4.59	-0.45	1.90	8.47	4.49	0.27	1.43	-0.34	1.63	0.20	0.35	3.00	10.24
2006	2.73	4.41	-1.00	1.79	3.71	4.76	-2.09	1.24	2.75	1.69	-0.19	0.43	13.62	9.99
2007	5.07	7.45	2.17	3.98	-4.95	7.88	-3.76	3.65	-4.44	1.99	0.56	0.91	3.53	15.93
2008	48.76	19.72	-7.63	15.00	69.26	23.97	21.52	20.28	-1.60	4.23	0.24	1.20	-38.49	40.81
2009	26.37	12.61	1.51	7.28	14.28	14.95	-1.38	10.48	11.38	5.35	1.18	1.18	24.71	27.18
Corr.	-0.50	0.99	-0.07	0.98	-0.73	0.99	-0.72	0.99	0.52	0.68	0.41	0.49		

VI. CONCLUDING REMARKS

In this study we verified that one can model the daily, high frequency dynamics of the S&P index on the basis of the scaling properties of the aggregated returns. The resulting martingale description generates histories whose statistical properties are consistent with those of the ensemble of daily histories on which the model has been calibrated. In the version of the model developed in this work the scaling property has been generalized with respect to previous formulations for FX rates returns [5], to describe the dynamics in a daily window of index evolution encompassing the whole trading session, and with the average volatility varying in a non-monotonous way. The martingale character of the model implies strictly zero linear correlation between elementary returns. This condition is only approximately verified within the dataset. Empirical estimations indeed show that the linear correlation is small, but nonzero, and changes sign as a function of time (see Fig. 9). On the other hand, we verified that our martingale model reproduces very well the more substantial nonlinear correlations.

The presence of these linear correlations suggests that the postulated daily process could present trends which, although difficult to model, may be exploited by appropriate trading strategies. Our choice has been then to use the martingale forecast capability of our model to define a trend-following strategy which reveals the presence of trends in the data in terms of a nonzero average profit. Besides the potential applicative interest on which we comment below, this result calls attention about the relevance that some apparently minor empirical features of the dynamics may have. In our case such a feature is a not strict satisfaction of the martingale character of the asset's dynamics, a

property which is often assumed in theoretical modeling.

Performing both in-sample and out-of-sample analyses we demonstrated how the scaling properties of the stochastic process can be used to derive long-term (intraday) density forecasts. In turns, these density forecasts can be used to define trading signals and to implement an intra-day trading strategy which exposes a small arbitrage opportunity. By comparing the trading outcomes to those obtained from a standard GARCH model, namely, the GJR [13], we showed better performances for the trading strategy based on the proposed model. The average trade profit is limited over the entire time span, even though local levels might be higher. Further studies aiming at improving the trading strategy and the empirical application of the model are thus required and under development.

Summarizing our findings, we can say that the proposed model has some potential for the development of trading strategies aimed at hedging the volatility risk, since their performances are positive during high market volatility, and characterized by a lower risk compared to the market index. Signals extracted from the model could also be considered as confirmatory signals for other strategies working with high frequency data, or could be used to detect relevant market movements.

In this empirical example we do not consider several elements that could have an impact on the trading strategy profits. We motivate this by the need of evaluating the model in comparison to a simple benchmark. Across the elements we did not include, we have the trading costs. Once those are introduced, the profits reported in the previous tables would be sensibly reduced. However, the trading strategy we implement is based on a fixed frequency database, using a 10-minute interval. This has a relevant impact on the trading outcomes. In fact, if a quantile violation is observed at time t , we execute the trade with the price observed at this same point in time. However, the violation could have taken place in any instant in the ten minutes before t . A trader using our approach would produce quantiles to be used for each period of 10 minutes, but would immediately detect the violation, and operate in the market soon after it (assuming she/he fully trusts the signal). On the contrary, working with a fixed time span of 10 minutes, we lose part of the potentially relevant content of the signal, since the price at time t might be significantly different from the real price observed at the trade execution just after the violation occurred.

Another element not included in our trading example is the remuneration of the bank account. In addition, overnight liquidity operations could be introduced given that the portfolio is entirely into cash from 16:00 p.m. of day t up to 10:09 a.m. of day $t + 1$. Finally, we note that even the trading strategy could be improved, for instance introducing stop-loss and take-profit bounds on the implemented orders.

Acknowledgments

We thank M. Zamparo for useful discussions. This work is supported by “Fondazione Cassa di Risparmio di Padova e Rovigo” within the 2008-2009 “Progetti di Eccellenza” program.

-
- [1] Admati, A. and Pfleiderer, P., A theory of intraday patterns: volume and price variability. *Review of Financial Studies*, 1988, **1**, (1), 3–40.
 - [2] Allez, R. and Bouchaud, J-P., Individual and collective stock dynamics: intra-day seasonalities. *New Journal of Physics*, 2011, **13**, 25010.
 - [3] Andersen, T.G. and Bollerslev, T., Intraday periodicity and volatility persistence in financial markets. *Journal of Empirical Finance*, 1997, **4**, 115–158.
 - [4] Andersen, T.G. and Bollerslev, T., Heterogeneous information arrivals and return volatility dynamics: uncovering the long run in high volatility returns. *Journal of Finance*, 1997, **LII 3**, 975–1005.
 - [5] Baldovin, F., Bovina, D., Camana, F. and Stella, A.L., Modeling the Non-Markovian, Non-stationary Scaling Dynamics of Financial Markets. In *Econophysics of order-driven markets* (1st edn), edited by F. Abergel, B. K. Chakrabarti, A. Chakraborti and M. Mitra, Part III, pp. 239–252, 2011 (New Economic Windows, Springer).
 - [6] Baldovin, F. and Stella, A.L., Scaling and efficiency determine the irreversible evolution of a market. *PNAS*, 2007, **104**, (50), 19741–19744.
 - [7] Bassler, K.E., McCauley, J.L. and Gunaratne, G.H., Nonstationary increments, scaling distributions, and variable diffusion processes in financial markets. *PNAS*, 2007, **104**, (44), 17287–17290.
 - [8] Bollerslev, T., Generalized autoregressive conditional heteroskedasticity. *Journal of Econometrics*, 1986, **31**, 307–327.
 - [9] Bouchaud, J-P. and Potters, M., *Theory of Financial Risk and Derivative Pricing* (2nd edn), Cambridge University Press, 2009.
 - [10] Clark, P.K., A Subordinated Stochastic Process Model with Finite Variance for Speculative Prices. *Econometrica*, 1973, **41**, (1), 135–155.
 - [11] Dacorogna, M.M., Gencay, R., Muller, A.U., Olsen, R.B., and Pictet, O.V., *An introduction to high frequency finance*, Academic Press, San Diego (2001).

- [12] Engle, R.F., Autoregressive conditional heteroskedasticity with estimates of the variance of U.K. inflation. *Econometrica*, 1982, **50**, 987–1008.
- [13] Glosten, L., Jagannathan, R. and Runkle, D., Relationship Between the Expected Value and the Volatility of the Nominal Excess Returns on Stocks. *Journal of Finance*, 1993, **48**, 1779–1801.
- [14] Guillaume, D.M., Dacorogna, M.M., Dave, R.R., Muller, A.U., Olsen, R.B., and Pictet, O.V., From the bird’s eye to the microscope: a survey of new stylized facts of the intra-daily foreign exchange market, *Finance and Stochastics* 1997, **1**, 95–129.
- [15] Mantegna, R.N. and Stanley, H.E., Scaling behaviour in the dynamics of an economic index. *Nature*, 1995, **376**, 46–49.
- [16] Miccichè, S., Bonanno, G., Lillo, F. and Mantegna, R.N., Volatility in financial markets: stochastic models and empirical results, *Physica A*, 2002, **314**, 756.
- [17] Mueller, U. A., Dacorogna, M., Olsen, R.B., Pictet, O.V., Schwarz, M. and Morgeneegg, C., Statistical study of foreign exchange rates, empirical evidence of a price change scaling law, and intraday analysis. *Journal of Banking & Finance*, 1990, **14**, (6), 1189–1208.
- [18] Neely, C.J., and Weller, P.A., Intraday technical trading in the foreign exchange market, *Journal of International Money and Finance*, Volume 22, Issue 2, April 2003, Pages 223-237.
- [19] Lo, A.W., H. Mamaysky, and J. Wang, Foundations of Technical Analysis: Computational Algorithms, Statistical Inference, and Empirical Implementation, *Journal of Finance*, 55(4), 1705-1770.
- [20] Park, C.H, and Scott, H., What do we know about the profitability of technical analysis? *Journal of Economic Surveys*, Volume 21, Issue 4, pages 786-826, 2007.
- [21] Peirano, P.P, Challet, D., Baldovin-Stella stochastic volatility process and Wiener process, *Eur. Phys. J. B*, 2012, **85**, 276.
- [22] Seemann, L., McCauley, J.L., Gunaratne G.H. Intraday volatility and scaling in high frequency foreign exchange markets, *International Review of Financial Analysis* Volume 20, Issue 3, June 2011, Pages 121-126, 2011.
- [23] Stella, A.L., Baldovin, F., Anomalous scaling due to correlations: Limit theorems and self-similar processes. *J. Stat. Mech.* P02018 (2010).
- [24] Wang, F., Yamasaki, K., Havlin, S., Stanley, H.E., Indication of multiscaling in the volatility return intervals of stock markets. *Phys. Rev. E* 77, 016109 (2008).
- [25] Wirjanto, T.S., and Xu, D., The Applications of Mixture of Normal Distributions in Finance: A Selected Survey. Working Paper, University of Waterloo, 2009.

Appendix: Testing linear and non-linear returns’ correlations

First of all we show that linear correlations on a 10-minute scale,

$$c_{lin}(t) \equiv \frac{\frac{1}{M} \sum_{l=1}^M r_1^{(l)} r_t^{(l)}}{\sqrt{\frac{1}{M} \sum_{l=1}^M (r_1^{(l)})^2} \sqrt{\frac{1}{M} \sum_{l=1}^M (r_t^{(l)})^2}}, \quad (36)$$

albeit absent in the model oscillate around ± 0.1 in the empirical data (see Fig. 9). These correlation are responsible for the presence of a trend which makes the presented strategy profitable. Due to their oscillating nature, it is difficult finding for them an appropriate modeling.

However, non-linear correlations represented for instance by the volatility autocorrelation,

$$c_{vol}(t) \equiv \frac{\frac{1}{M} \sum_{l=1}^M |r_1^{(l)}| |r_t^{(l)}| - \left(\frac{1}{M} \sum_{l=1}^M |r_1^{(l)}| \right) \left(\frac{1}{M} \sum_{l=1}^M |r_t^{(l)}| \right)}{\frac{1}{M} \sum_{l=1}^M |r_1^{(l)}|^2 - \left(\frac{1}{M} \sum_{l=1}^M |r_1^{(l)}| \right)^2}, \quad (37)$$

are a stronger and much more stable feature which is well reproduced by our model during both the morning and the afternoon trading sessions (see Fig. 10, where the parameters derived from the in-sample analysis have been used).

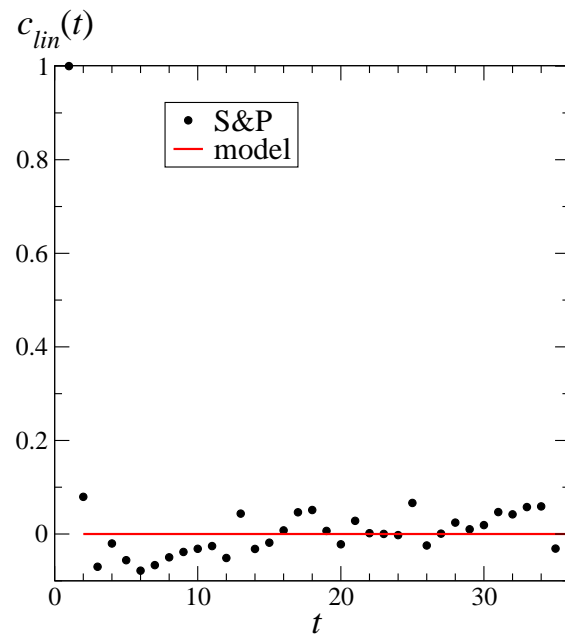


FIG. 9: Linear correlation

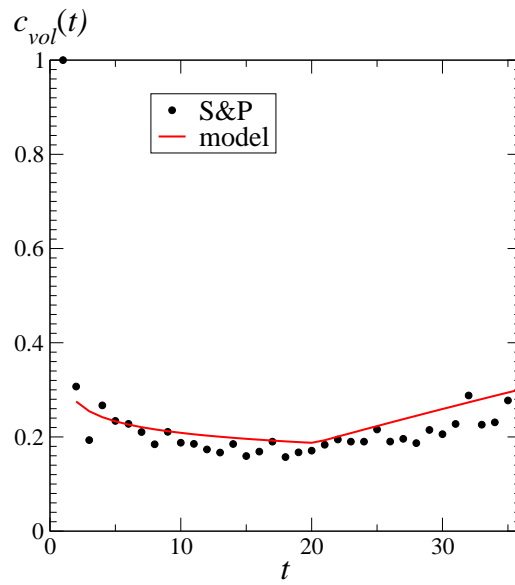


FIG. 10: Volatility autocorrelation.